第 27 卷第 4 期 无 机 化 学 学 报 Vol.27 No.4
2011 年 4 月 CHINESE JOURNAL OF INORGANIC CHEMISTRY 747-751

氧化铁薄膜的水热合成及其光电转换性能

万丽娟[1,3] 王治强[1] 杨再三[1] 罗文俊[1,3] 李朝升*[,1,2,3] 邹志刚[1,2,3]
([1]南京大学环境材料与再生能源研究中心,南京大学物理系,南京 210093)
([2]南京大学材料科学与工程系,南京 210093)
([3]南京大学固微结构物理国家重点实验室,南京 210093)

摘要: 通过水热方法在掺杂氟的 SnO_2(FTO)导电玻璃上制备了不同形貌的氧化铁薄膜。利用无机铁盐浸渍法在 FTO 玻璃上进行氧化铁晶种的预处理使得所制备的氧化铁薄膜更致密且均一。研究了表面活性剂对氧化铁晶体形貌的影响。使用十二烷基苯磺酸钠(SDBS)和三嵌段聚合物 P123 做为形貌导向剂分别得到棒状和四方体形貌的氧化铁薄膜。氧化铁薄膜可调的形貌可能是由于表面活性剂和铁氧团簇的组装或者某些晶面吸附了阴离子而改变了生长速率引起的。同时,研究了其光电性能,具有四面体形貌的氧化铁薄膜可以产生较大的光电流,这是由于其缩短了光生空穴的扩散距离。

关键词: 氧化铁; 水热; 薄膜; 光电化学
中图分类号: O614.24 **文献标识码**: A **文章编号**: 1001-4861(2011)04-0747-05

Seed-Mediated Hydrothermal Synthesis and Photoelectrochemical Properties of Hematite Thin Films

WAN Li-Juan[1,3] WANG Zhi-Qiang[1] YANG Zai-San[1] LUO Wen-Jun[1,3] LI Zhao-Sheng*[,1,2,3] ZOU Zhi-Gang[1,2,3]
([1]*Eco-Materials and Renewable Energy Research Center (ERERC), Department of Physics, Nanjing University, Nanjing* 210093, *china*)
([2]*Department of Materials Science and Engineering, Nanjing University, Nanjing* 210093, *china*)
([3]*National Laboratory of Solid State Microstructures, Nanjing University, Nanjing* 210093, *china*)

Abstract: Iron oxides with different morphologies on F-doped tin oxide (FTO) covered glass substrates were synthesized through hydrothermal route. The pretreatment of iron oxide crystalline seeds on FTO glass through inorganic iron salts solution dipping method makes the as-prepared iron oxide thin films more uniform and compact. The effects of surfactants on the crystal morphologies of iron oxides were studied. Uniform iron oxides thin films with rod-like and tetrahedral morphologies could be obtained through this route by using dodecylbenzensulfonate (SDBS) and triblock copolymer P123 as morphology directing-agent, respectively. The modulated morphologies of iron oxide thin films may be attributed to the assembly between surfactant and ferric oxo-clusters or different velocity of crystalline facets growth induced by adsorbed anions. Photoelectrochemical properties of iron oxide thin films with different morphologies were studied. The larger values of produced photocurrents of iron oxide thin films with tetrahedral morphology may be attributed to the minimization of the diffuse distance for photogenerated holes.

Key words: iron oxide; hydrothermal; thin films; photoelectrochemical properties

Since the hydrogen production from the direct photo electrolysis of water was first demonstrated by Fujishima and Honda[1], conversion of solar energy to hydrogen as a clean and renewable energy source has

收稿日期:2010-09-15。收修改稿日期:2010-11-01。
973(No.2007CB613305),国家自然科学基金(No.50732004),江苏省自然科学基金(No.BK2008028)资助项目。
*通讯联系人。E-mail:zsli@nju.edu.cn

received more attention. The classical work shows that it is possible to induce the water-splitting by light, using TiO_2 semiconductor as photoanode. However, TiO_2 has a wide band gap (3.2 eV), and only a small fraction of the solar spectrum (light below 420 nm) can be utilized. Therefore the main interest of the present study is focused on the shift of activity of photoanode materials to the visible region of sunlight[2-4].

Iron oxide (α-Fe_2O_3, or hematite) with a favorable band gap of 2.0~2.2 eV remains a promising material, due to its chemical stability in aqueous environments and matchless abundance [5]. Thin-films Fe_2O_3 photoanodes has been reported fabrication through several methods, including spin coating [6]; DC magnetron sputtering [7]; atmospheric pressure chemical vapor deposition (APCVD)[8]; spray pyrolysis of Fe(III)-containing solutions[9] etc. Hydrothermal route has been widely used in the synthesis of semiconductor thin films on different substrates[10-12], which is a facile method and the products morphologies may be controlled by additives, e.g., anions or surfactant. To the best of our knowledge, there have been no reports on α-Fe_2O_3 thin films prepared through hydrothermal route.

We report here the synthesis of different morphologies of α-Fe_2O_3 thin films by hydrothermal route, using ferric chloride as inorganic precursor, dodecylbenzensulfonate (SDBS) and triblock copolymer P123 as morphology directing-agent, respectively. In the hydrothermal system, crystalline seeds of iron oxides on FTO (F-doped tin oxide) substrates make the as-prepared α-Fe_2O_3 thin films more uniform and compact, compared with those films on FTO substrates without crystalline seeds treatment. The photoelectrochemical properties of α-Fe_2O_3 thin films with different morphologies are also reported.

1 Experimental

1.1 Preparation of Fe_2O_3 films

All reagents were of analytical grade and used without further purification. Manipulations and reactions were carried out in air without the protection of nitrogen or inert gas. FTO glass substrates were washed with ethanol and water several times before use. To get the FTO covered with iron oxides crystalline seeds, the substrates were dipped in the ferric nitride ethanol solution for several times, then dried and calcined at 500 ℃ for 4 h. In a typical run, 1.621 7 g of $FeCl_3 \cdot 6H_2O$ was added into 35 mL of deionized water and stirred until totally dissolved. The reaction solution was then transferred into a 50 mL Teflon-lined stainless steel autoclave. The FTO substrates (1.5 cm×2 cm) were put on the bottom of Teflon-lined stainless steel autoclave. The autoclave was sealed and heated to 200 ℃ and kept for 2 h ($FeCl_3+H_2O \rightarrow Fe_2O_3+HCl$). After being cooled down to room temperature naturally, the as-prepared iron oxides thin films/FTO were washed with deionized water and absolute ethanol several times. In order to study the effects of surfactants, 0.2 g dodecylbenzensulfonate (SDBS) or 0.5 g $(EO)_{20}(PO)_{70}(EO)_{20}$ (P123) was added into the reaction solution with other conditions unchanged.

1.2 Characterization

X-ray diffraction (XRD) measurements were performed on a Rigaku D/MAX-Ultima III X-ray diffractometer with Cu $K\alpha$ radiation (λ=0.154 18 nm, 40 kV, 40 mA), flash detector, graphite monochromator and a scan rate of $10° \cdot min^{-1}$ (scan range: 20°~60°, CPS type of X-ray recording). UV-Vis transmission spectra were performed at Varian Cary 50 Probe UV-Visible Spectrophotometer. Morphologies of the as-prepared samples at different experimental conditions were characterized by scanning electron microscopy (SEM) Philips XL30 with an electron accelerating voltage of 10 kV.

The photoelectrochemical properties were characterized by linear scanning voltampere (LSV) technique performed on a CHI633C electrochemical workstation system with 500W xenon lamp (USHIO Optical Module X500) illumination. The LSV measurements were performed in a 1 $mol \cdot L^{-1}$ NaOH aqueous solution from −0.30 to 0.40 V with a scan rate of 20 $mV \cdot s^{-1}$ in a standard three-electrode configuration coupled with the sample films (working electrode), an Ag/AgCl electrode (reference electrode) and a high purity platinum (counter electrode).

2 Results and discussion

Wide-angle XRD pattern of the as-prepared samples is shown in Fig.1. As seen from Fig.1, with the exception of the marked FTO glass substrate peaks, the XRD data is consistent with the rhombohedral symmetry of Fe_2O_3 (space group: $R3c$ (167), a=0.503 5 nm, b=0.503 5 nm and c=1.374 8 nm; PDF card No. 33-0664) indicating the presence of α-Fe_2O_3 structure and absence of impurity phases. The inset digital photograph in Fig.1 shows the as-prepared hematite films is uniform and transparent in a large scale, suggesting that α-Fe_2O_3 films can be synthesized on the crystalline seed-treated FTO glass substrates successfully through hydrothermal treatment in a simple inorganic iron salt system.

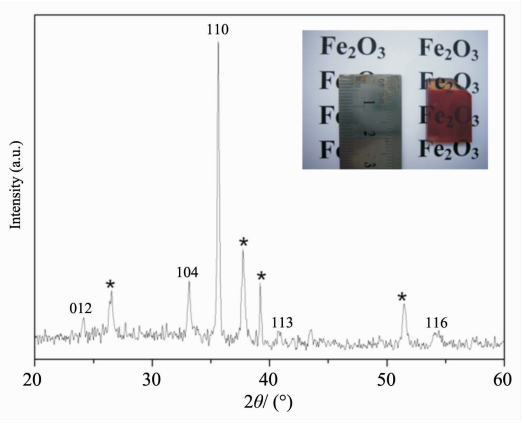

* (represent FTOs diffraction peaks). Inset is the digital photo of transparent iron oxide films

Fig.1　XRD pattern of iron oxide/FTO films

The morphologies of the as-prepared α-Fe_2O_3 films are characterized by SEM observation in Fig.2. Fig.2 (a) and (b) show the relatively uniform iron oxide films, and there are no obvious cracks. When the reaction solution was added with surfactant SDBS, the morphology of as-prepared iron oxide thin films appears different from that without surfactant. It seems more uniform with rod-like morphology (Fig.3a, inset is the magnified SEM image). When triblock copolymer P123 was used as morphology-directing agent, the iron oxide thin films with connected tetrahedral morphology was observed (Fig.3b, inset is the magnified SEM image). The modulated morphologies of iron oxide thin films may be

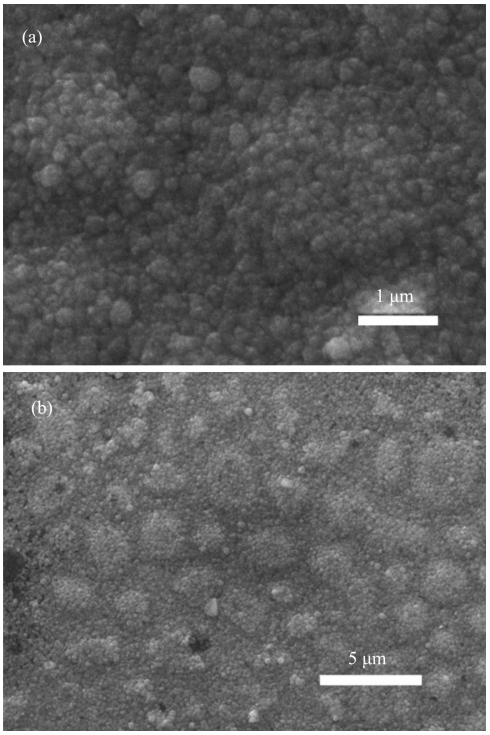

(a) low magnification image; (b) high magnification image

Fig.2　SEM image of iron oxide/FTO films prepared in ferric chloride

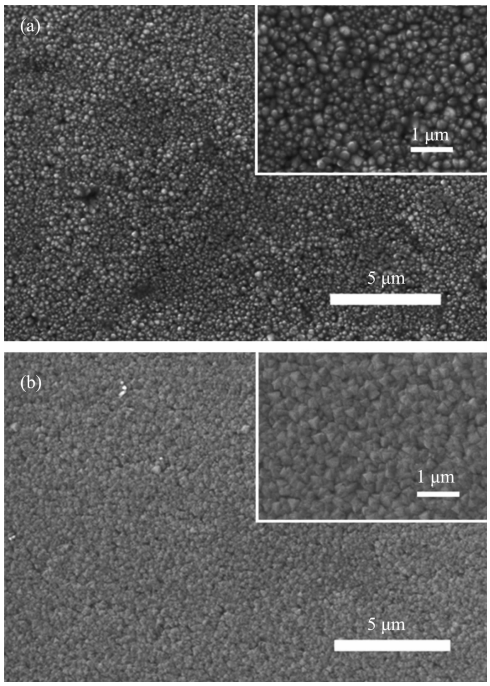

(a) SDBS; (b) P123

Fig.3　SEM image of iron oxide/FTO films prepared in ferric chloride with surfactant

attributed to the assembly between surfactant and ferric oxo-clusters. For the samples produced from SDBS,

some crystalline facets may be adsorbed by the anions during the crystal growth of iron oxides. While for the samples from P123, ferric oxo-clusters may be interacted with the copolymer to form iron oxide with tetrahedral morphology.

Fig.4 shows transmittance spectra for the as-prepared Fe_2O_3 films with different morphologies. The optical band gap of films can be estimated by calculating the intercept of the extrapolated linear fit to the experimental data of a plot of $(-\ln T)^n$ (T is the transmittance value, n is 1/2 for hematite, as hematite is known to be indirect band gap semiconductor) versus incident photon energy ($h\nu$), which can be seen from the insets of Fig.4. The insets show the indirect band gap values of all films are about 2.0 eV, which is consistent with the values of the samples prepared through atmospheric pressure chemical vapor deposition and USP (Ultrasonic Spray Pyrolysis). reported in the literature[5,13].

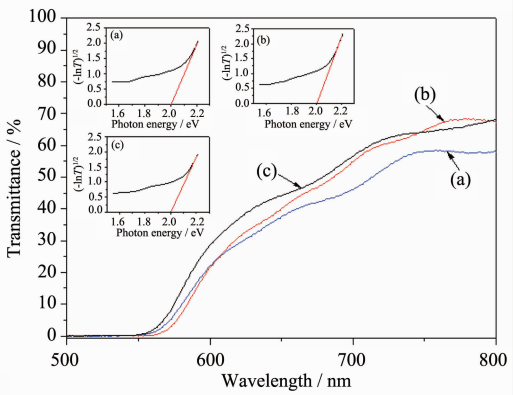

(a) without surfactant; (b) SDBS; (c) P123. Inset are $(-\ln T)^{1/2}$ vs. photon energy ($h\nu$) plots for corresponding films. The optical band gap is determined by extrapolation

Fig.4 Transmittance spectra of the as-prepared samples

Fig.5 shows the photocurrent curves of the iron oxide thin films with different morphologies. The photocurrent of Fe_2O_3 thin films with tetrahedral morphologies is larger than others, which may be in part attributed to the nanostructure. The morphologies of iron oxide thin films may influence the photoelectrochemical properties, e.g. the improvement of photocurrent of the iron oxide films may be attributed to the change of nanostructures (smaller grains), which improved photocurrent is in part attributed to the

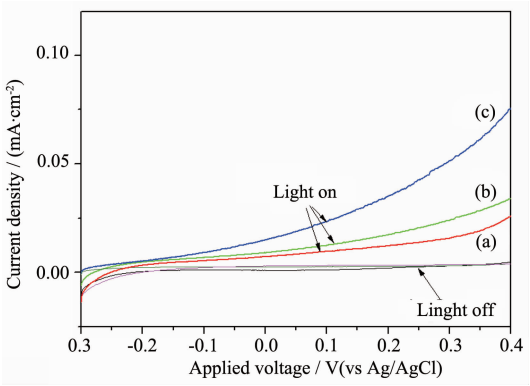

(a) without surfactant; (b) SDBS; (c) P123

Fig.5 Photocurrent-voltage curves for iron oxide electrodes in darkness and under illumination at a scan rate of 20 $mV \cdot s^{-1}$

dendritic nanostructure which minimizes the distance photogenerated holes have to diffuse to reach the Fe_2O_3/electrolyte interface while still allowing efficient light absorption [7-8]. The improved photocurrent of as-prepared iron oxide thin films with tetrahedral morphology may be attributed to minimize the distance photogenerated holes of diffusion.

3 Conclusions

Different morphologies of α-Fe_2O_3 thin films were synthesized by hydrothermal route, using ferric chloride as inorganic precursor, SDBS and P123 as morphology directing-agent. The rod-like and tetrahedral morphologies were obtained. Crystalline seed of iron oxide on FTO substrate make the as-prepared α-Fe_2O_3 thin films more uniform and compact compared with those FTO without pretreatment. The photocurrent of Fe_2O_3 thin films with tetrahedral morphologies is larger than others, which may be attributed to the tetrahedral morphology in minimization of the diffuse distance of photogenerated holes.

References:

[1] Fujishima A, Honda K. *Nature*, **1972**,**238**:37-38
[2] Park J H, Kim S, Bard A. *J. Nano Lett.*, **2006**,**6**:24-28
[3] Matsuoka M, Kitano M, Takeuchi M, et al. *Catal. Today*, **2007**,**122**:51-61
[4] Mor K G, Prakasam H E, Varghese O K, et al. *Nano Lett.*, **2007**,**7**:2356-2364

[5] Cesar I, Sivula K, Kay A, et al. *J. Phys. Chem. C*, **2009**,**113**: 772-782

[6] Souza F L, Lopes K P, Longo E, et al. *Phys. Chem. Chem. Phys.*, **2009**,**11**:1215-1219

[7] Glasscock J A, Barnes P R F, Plumb I C, et al. *J. Phys. Chem. C*, **2007**,**111**:16477-16488

[8] Kay A, Cesar I, Grätzel M. *J. Am. Chem. Soc*., **2006**,**128**: 15714-15721

[9] Sartoretti C J, Alexander B D, Solarska R, et al. *J. Phys. Chem. B*, **2005**,**109**:13685-13692

[10]Chen J, Huang K L, Liu S Q. *Electrochimica Acta*, **2009**,**55**: 1-5

[11]Na J S, Gong B, Scarel G, et al. *ACS Nano*, **2009**,**3**:3191-3199

[12]Zhao H J, Shen Y M, Zhang S Q, et al. *Langmuir*, **2009**,**25**: 11032-11037

[13]Duret A, Grätzel M. *J. Phys. Chem. B*, **2005**,**109**:17184-17191